ELSEVIER

Journal of Nuclear Materials 247 (1997) 63–71

journal of nuclear materials

Section 3. Basic properties

Thermochemistry of IVA transition metal–oxygen solid solutions

Toshihide Tsuji *

Department of Nuclear Engineering, Faculty of Engineering, Nagoya University, Furo-cho, Chikusa-ku, Nagoya 464-01, Japan

Abstract

The α-phase of IVA transition metals namely, titanium, zirconium and hafnium, dissolves oxygen atoms up to 33 at.% (O/Ti = 0.49), 29 at.% (O/Zr = 0.41) and 20 at.% (O/Hf = 0.25) at room temperature, respectively, in the octahedral interstitial site of hcp metal lattice. At low temperatures, the dissolved oxygen atoms form the completely ordered structures at higher oxygen to metal ratios. The completely ordered crystal structure transforms to the completely disordered phase, through partially ordered phase at high temperatures, depending on the transition metal and composition. The phase diagrams in the Ti–O, Zr–O and Hf–O solid solutions determined from the peak temperature by heat capacity measurement are shown. The experimental transition entropy changes of the order–disorder transition for HfO_x and TiO_x obtained by heat capacity measurement are compared with the theoretical values calculated on the basis of the crystal structure analysis by using statistical thermodynamics and discussed. © 1997 Elsevier Science B.V.

1. Introduction

Various elementary models (Ising model, Bragg–Williams model and the cluster variation method proposed by Kikuchi [1]) have been proposed to understand the order–disorder transition behavior of binary substitutional alloys. These models are evaluated for binary body-(β-CuZn) and face-centered cubic lattices (Cu_3Au) by comparing the calculated entropies with the experimental ones. Among these models, the cluster variation method is a good model to explain the order–disorder transition of binary substitutional alloys [2]. On the other hand, for binary interstitial alloys, the solubility of interstitial atoms to metals is normally so small that the interstitial atoms do not form order structures. Thus, the elementary models of order–disorder transition for binary interstitial alloys are lacking. However, the α-phases of IVA transition metals namely, titanium, zirconium and hafnium, dissolve a large amount of oxygen atoms in the octahedral interstitial sites of hcp metal lattices. It is expected that the oxygen atoms dissolved in titanium, zirconium and hafnium metals form ordered structures at higher oxygen to metal ratios in low temperatures and cause the order–disorder transition at higher temperatures. Therefore, the Ti–O, Zr–O and Hf–O solid solutions are good systems to compare the experimental transition entropy changes with the theoretical values.

2. Phase diagrams of Ti–O, Zr–O and Hf–O systems

Phase diagrams of the Ti–O, Zr–O and Hf–O systems taken from 'Binary alloy phase diagrams' are shown in Figs. 1–3, respectively [3]. As seen in Figs. 1–3, the α-phases of titanium, zirconium and hafnium dissolve oxygen atoms up to 33 at.% (O/Ti = 0.49), 29 at.% (O/Zr = 0.41) and 20 at.% (O/Hf = 0.25), respectively, in the octahedral interstitial sites of hcp

* Tel.: +81-52 789 3776; fax: +81-52 789 4685; e-mail: t-tsuji@nucl.nagoya-u.ac.jp.

PII S0022-3115(97)00064-0

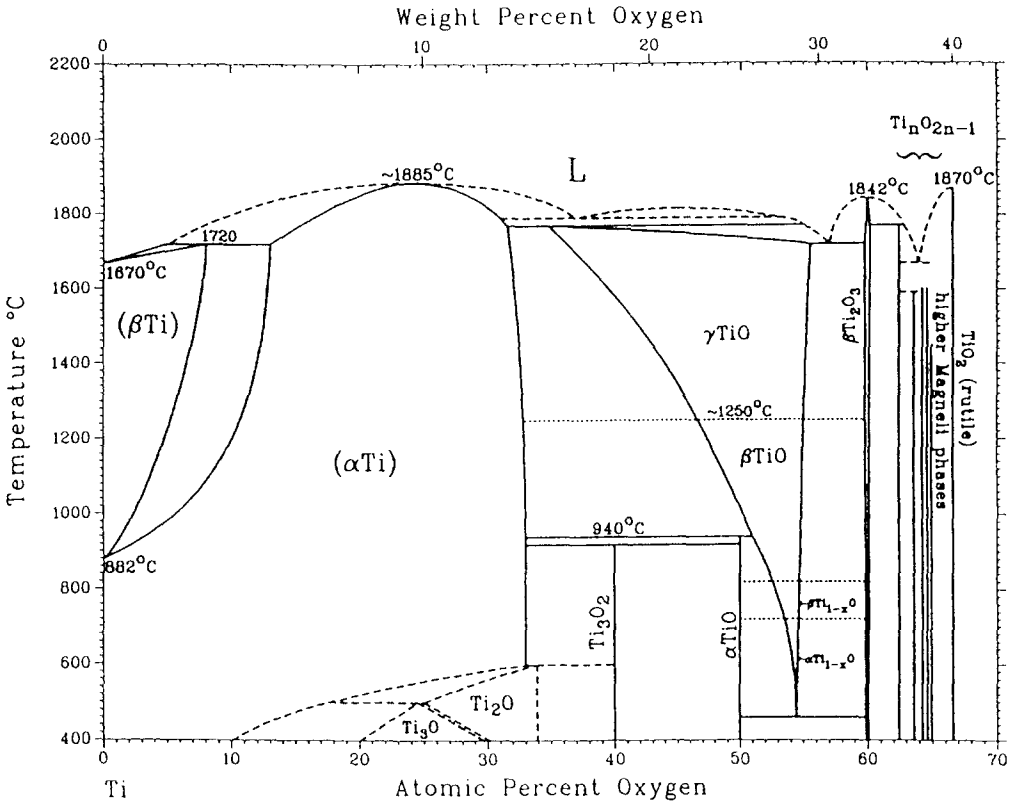

Fig. 1. Phase diagram in the Ti–O system [3].

metal lattices. At low temperatures, the dissolved oxygen atoms form ordered structures at higher oxygen to metal ratios ($0.10 < x < 0.49$ for TiO_x, $0.10 < x < 0.41$ for ZrO_x, $0.10 < x < 0.25$ for HfO_x), and these ordered phases transform to the disordered phases between 600 and 800 K, as will be discussed later. Since the solubility limit of oxygen atoms dissolved in hafnium metal is smaller than those in titanium and zirconium metals, a more simple ordered structure is expected for the Hf–O solid solution. The crystal structures of the ordered phases in the Ti–O, Zr–O and Hf–O systems at low temperatures have been determined by X-ray, neutron and electron diffraction methods as will be shown below. However, the existing ranges of these ordered phases for Ti–O and Zr–O systems at low temperatures are uncertain and are shown in the dotted or broken lines in Figs. 1 and 2, respectively. For the Hf–O system, the ordered phase at low temperatures is not shown in Fig. 3. Therefore, the existing ranges of the ordered phases in the Ti–O, Zr–O and Hf–O systems at low temperatures determined by heat capacity measurements in this study will be shown later.

It is also seen in Figs. 1–3 that the transition temperature from α- to β-phase in hafnium metal (2016 K) is higher than those in titanium (1155 K) and zirconium (1136 K) metals. Thus, it is considered that the α-phase of hafnium is more stable than those of titanium and zirconium.

3. Ordered crystal structures of TiO_x, ZrO_x and HfO_x

Oxygen atoms dissolved in the α-phase of titanium, zirconium and hafnium metals having the hexagonal closed packing occupying three kinds of the octahedral sites (A, B and C sites) of hcp, as seen in Fig. 4. The ordered crystal structures are distinguished by different ways of the oxygen occupancy of the three kinds of octahedral interstitial sites in a plane perpendicular to the c-axis and the stacking sequences of the planes parallel to the c-axis. The ordered crystal structures of TiO_x [4], ZrO_x [5] and HfO_x [6] have been determined by X-ray, neutron and electron diffraction methods. The ordered structures of TiO_x, ZrO_x and HfO_x are shown in Figs. 5–7, respectively, where only oxygen atom sites are depicted. For

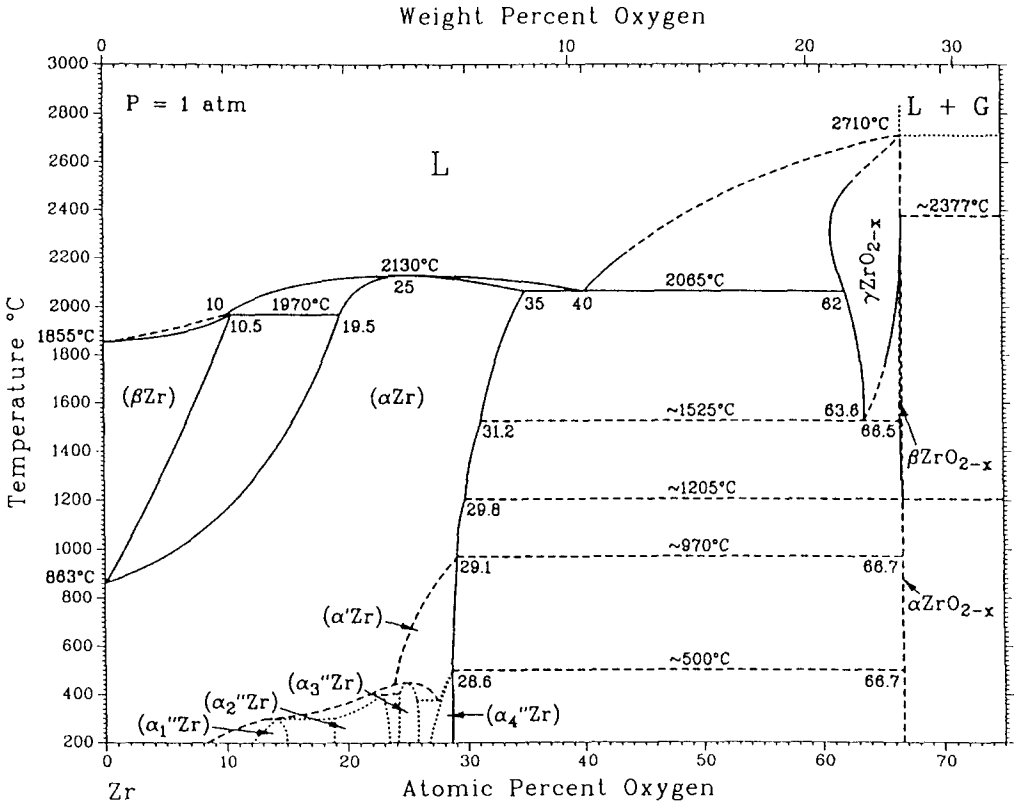

Fig. 2. Phase diagram in the Zr–O system [3].

TiO_x, oxygen sublattices of the completely ordered Ti_6O(a), Ti_3O(b) and Ti_2O(c) and that of the partially ordered α'-Ti_2O(d) are shown in Fig. 5 [4]. Hirabayashi [5] determined the ordered crystal structures of ZrO_x ($x \sim 1/3$) (a), ZrO_z ($z \sim 1/2$) (b) and ZrO_y ($y \sim 1/3$) (c) and the ordered structures are shown in Fig. 6. In HfO_x the basic completely ordered

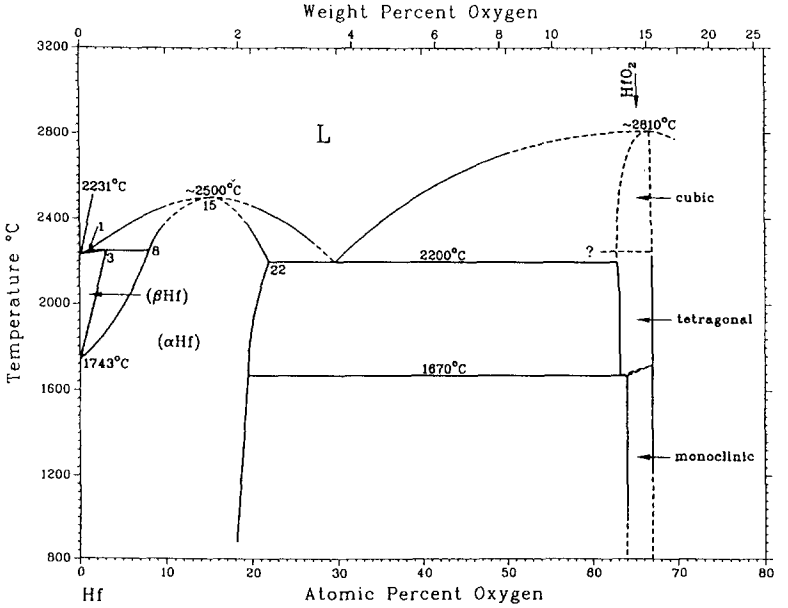

Fig. 3. Phase diagram in the Hf–O system [3].

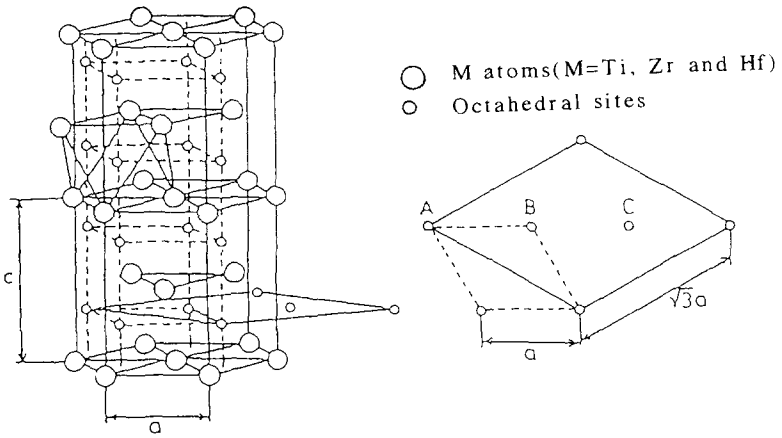

Fig. 4. Octahedral sites of hcp for IVA transition metal.

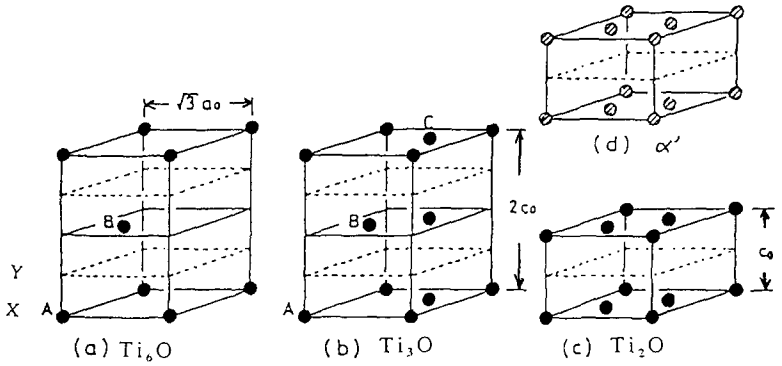

Fig. 5. Oxygen sublattices of Ti_6O(a), Ti_3O(b), Ti_2O(c) and α′-Ti_2O(d). The C sites in (d) are partially filled.

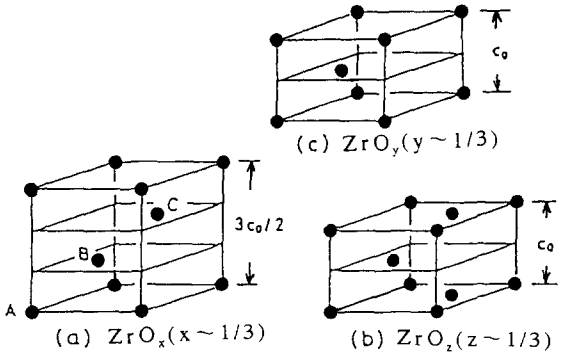

Fig. 6. Oxygen sublattices of ZrO_x(a), ZrO_z(b) and ZrO_y(c).

structure is the ordered one for $x = 1/6$, and oxygen vacancies for $x \leq 1/6$(a) or the interstitial oxygen atoms for $x > 1/6$(b) exist in the basic ordered structure [6].

For ZrO_x, as seen in Fig. 6, every layer perpendicular to the c-axis is occupied by interstitial oxygen atoms, whereas every second layer is vacant for TiO_x in Fig. 5 and for HfO_x in Fig. 7. This can be explained by the fact that the c-axis of

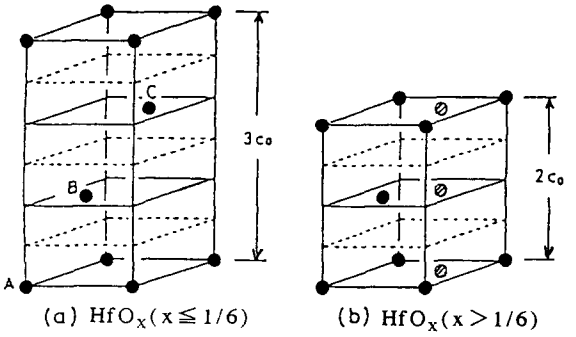

Fig. 7. Oxygen sublattices of HfO_x ($x \leq 1/6$)(a) and HfO_x ($x > 1/6$)(b).

unit cell for the zirconium (0.515 nm) is larger than those for titanium (0.468 nm) and hafnium (0.505 nm) and more space is available for oxygen atoms for ZrO_x.

4. Heat capacity data by adiabatic scanning calorimeter

Heat capacity measurement is a very powerful technique to obtain the transition temperature and transition entropy change due to the order–disorder of interstitial oxygen atoms in TiO_x, ZrO_x and HfO_x alloys. Heat capacities of α-MO_x (M = Ti, Zr and Hf) were measured from 325 to 905 K by our group [7–11] as well as Hirabayashi's group [5,12,13] using an adiabatic scanning calorimeter [14] and automatic adiabatic calorimeter [15], respectively. Typical heat capacity data of $HfO_{0.17}$ measured by our group are shown in Fig. 8 as a function of temperature [11]. A heat capacity anomaly is observed around 730 K, and assigned to an order–disorder rearrangement of oxygen atoms. Similar heat capacity anomalies due to the order–disorder transition were observed around 700 K for all the Hf–O solid solutions [11,16].

In Fig. 8, another heat capacity anomaly is seen in the lower temperature range up to 600 K. Similar heat capacity anomalies have been observed for titanium–oxygen [7], zirconium–oxygen [8–10] and hafnium–oxygen [11,16] solid solutions, and these anomalies have made the estimation of the experimental transition entropy changes difficult. The appearance of the low temperature heat capacity anomaly is considered to be caused by lowered helium gas pressure on annealing the sample which led to insufficient heat conduction in a quartz vessel. The details of this mechanism are discussed in another paper of this conference [16]. We could not examine the reason why helium gas pressure lowered during annealing the sample. Considering that IVA transition metals dissolve a large amount of light elements, e.g., hydrogen, carbon, nitrogen and oxygen, some of helium gas may be absorbed in hafnium–oxygen solid solution during annealing the sample.

In order to compute the experimental transition entropy changes from heat capacity data in this study, the appropriate

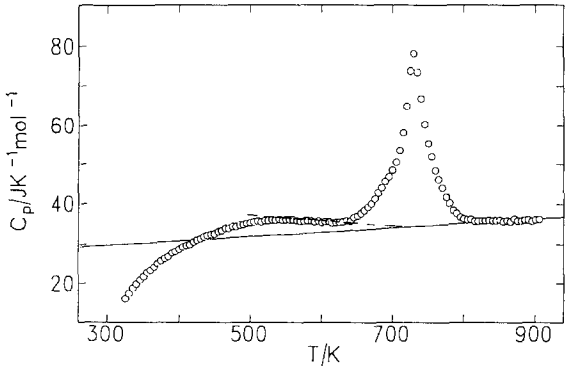

Fig. 8. Heat capacity data of $HfO_{0.17}$ as a function of temperature.

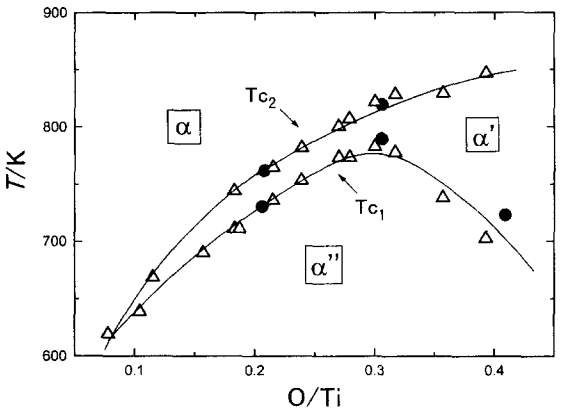

Fig. 9. Order–disorder transition temperature of TiO_x against O/Ti ratio. ●: Tsuji et al. [7,17], △: Koiwa and Hirabayashi [12].

peak area due to the order–disorder transition has to be determined excluding the effect of the low temperature heat capacity anomaly. As seen in Fig. 8, two lines are required to determine transition entropy change. One is the decreasing line of the low temperature heat capacity anomaly and the other is the base line of the heat capacity curve. The decreasing line of the low temperature heat capacity anomaly is determined by fitting heat capacity data to the straight line in the appropriate part of the anomaly, and the fitting line is shown as the dotted line in Fig. 8. The base line in Fig. 8 is determined by curve fitting heat capacity data excluding the heat capacity anomaly due to the order–disorder transition to a straight line and is shown as the solid line. Now, we can obtain the experimental transition entropy change by integrating on the area enclosed by heat capacity curve, the decreasing line shown as the dotted line and the base line shown as the solid line in Fig. 8.

The new phase diagram of the α-phase for Ti–O [7,12], Zr–O [10,13] and Hf–O [6,11,16] systems determined by heat capacity measurements in this study are shown in Figs. 9–11, respectively. In these figures, other literature values are also shown for comparison. The transition temperatures determined in this study are in good agreement with those obtained by other investigators. For the Hf–O solid solution, as seen in Fig. 11, the order–disorder transition occurs directly from the completely ordered phase (α″) to the completely disordered one (α). On the other hand, the partially ordered phase (α′) exists between the completely ordered and the completely disordered phases in the titanium- and zirconium–oxygen solid solutions, as seen in Figs. 9 and 10. For the Zr–O system in Figs. 2 and 10, the completely ordered phases (α″) are further divided into $ZrO_{1/6}$ (α''_1), ZrO_x (α''_2), LPSS (α''_3) and ZrO_z (α''_4), where LPSS is the long period stacking structure, and the partially disordered phase is represented as ZrO_y (α′). In Fig. 9 phase boundaries of α″-Ti_3O and α″-Ti_2O are still

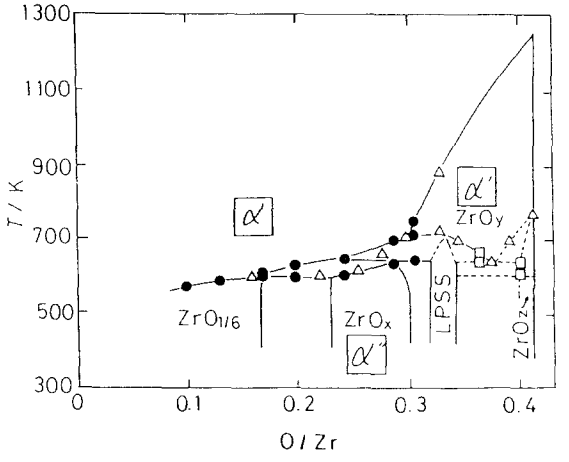

Fig. 10. Order–disorder transition temperature of ZrO_x against O/Zr ratio. ●: Tsuji and Amaya [10], △: Arai and Hirabayashi [13].

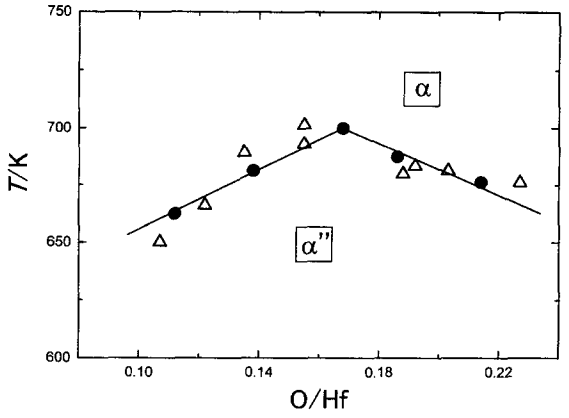

Fig. 11. Order–disorder transition temperature of HfO_x against O/Hf ratio. ●: Kato and Tsuji [11,16], △: Hirabayashi et al. [6].

uncertain. Phase boundaries of α″- and α′- and α-phases corrected for the Ti–O system in Fig. 1 and those for the Zr–O system in Fig. 2 are shown in Figs. 9 and 10, respectively.

5. Comparison between theoretical and experimental transition entropy changes

5.1. Hf–O

The theoretical and experimental transition entropy changes of HfO_x are shown in Fig. 12 as a function of the O/Hf ratio [6,11,16]. In Fig. 12, we can calculate the theoretical transition entropy changes by using statistical thermodynamics from configurational entropy changes for the interstitial oxygen atoms in the host hafnium lattice between the ordered and disordered phases, on the basis of crystal analyses. The equations used for the calculation are as follows [18]:

$$\begin{aligned} \Delta S_1 &= k\{\ln({}_{N-NX}C_{NX})\} - k\{\ln({}_{N/6}C_{NX})\}, && \text{for } X \le 1/6, \\ \Delta S_2 &= k\{\ln({}_{N-NX}C_{NX})\} - k\{\ln({}_{NX}C_{N\{X-(1/6)\}})\}, && \text{for } X > 1/6, \end{aligned} \tag{1}$$

where k and N are Boltzmann's constant and Avogadro's number, respectively. On the right hand side in these equations, the first and second terms are derived from the configurational entropies of the completely disordered and the completely ordered phases, respectively (model 1 by Koiwa and Hirabayashi [18]). In Eq. (1) the first term can be calculated by

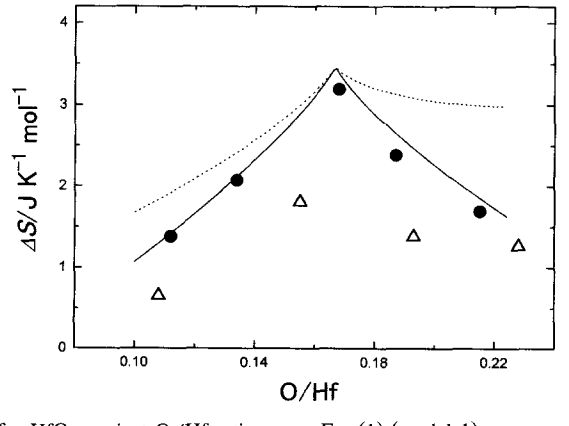

Fig. 12. Transition entropy changes for HfO_x against O/Hf ratio. · · ·: Eq. (1) (model 1), ————: Eq. (2) (model 2), ●: Kato and Tsuji [11,16], △: Hirabayashi et al. [6].

assuming that an oxygen atom is situated in an octahedral site, where at least two neighboring sites (above and below the first one) along the c-axis can not be filled with other atoms to avoid the closest oxygen-pairs with the distance $c_0/2$. The theoretical value is shown as the dotted line in Fig. 12. The experimental transition entropy change for the composition of $x = 0.17$ is in good agreement with the theoretical value. This fact implies that the order–disorder transition takes place by following the transition mechanism on the basis of the crystal analyses for the composition of $x = 1/6$ and the hafnium–oxygen solid solution for $x = 1/6$ has such a complete ordered structure as reported by Hirabayashi et al. [6].

On the other hand, the experimental transition entropy changes for other compositions ($x \neq 0.17$) are smaller than the theoretical values. We propose the increasing degree of configurational freedom of the ordered structure as one of explanations for the difference between the experimental and theoretical transition entropy changes (model 2 by us [16]). Assuming that factor 'a' is the number of the increasing degree per one oxygen vacancy for $x \leq 1/6$ (or one interstitial oxygen atom for $x > 1/6$), compared to the basic ordered structure for $x = 1/6$, the equations for the transition entropy change are expressed as

$$\begin{aligned} \Delta S_3 &= k\{\ln({}_{N-NX}C_{NX})\} - k\{\ln({}_{N/6}(C_{NX})a^{N\{(1/6)-X\}}\}, && \text{for } X \leq 1/6, \\ \Delta S_4 &= k\{\ln({}_{N-NX}C_{NX})\} - k\{\ln({}_{NX}C_{\{NX-(1/6)\}})a^{N\{X-(1/6)\}}\}, && \text{for } X > 1/6. \end{aligned} \tag{2}$$

The transition entropy changes calculated using these equations in the case of $a = 3$ for $x \leq 1/6$ and $a = 17$ for $x > 1/6$ are shown as the solid lines in Fig. 12. The composition dependence of the calculated transition entropy changes fits very well to the experimental values. We can not discuss, in more details, the order–disorder transition mechanism. However, it can be remarked that the interstitial oxygen atoms or the oxygen vacancies, compared to the basic ordered structure for $x = 1/6$, break the balance of the strong repulsive force between the interstitial oxygen atoms in hafnium metal, affect the configuration of the oxygen atoms originally occupying the interstitial sites in the basic ordered structure for $x = 1/6$, and then cause the increasing degree of configurational freedom of the ordered structure.

5.2. Ti–O

The theoretical and experimental transition entropy changes of TiO_x are shown in Fig. 13 as a function of O/Ti ratio [7,12,17]. In Fig. 13, we can calculate the theoretical transition entropy changes from configurational entropy changes for the interstitial oxygen atoms in host titanium lattice between the completely ordered and the partially ordered phases (ideal inter-plane disordering), on the basis of crystal analyses. The equations used for the calculation are as follows:

$$\begin{aligned} \Delta S_5 &= (-Nk/6)\{-6x\ln 3 + 3(1-2x)\ln(1-2x) - (1-6x)\ln(1-6x)\}, && \text{for } 0 < X \leq 1/6, \\ \Delta S_6 &= (-Nk/6)\{6x\ln 2x + 3(1-2x)\ln(1-2x) - (6x-1)\ln(6x-1) - (2-6x)\ln(2-6x)\}, && \text{for } 1/6 \leq X \leq 1/3 \\ \Delta S_7 &= (-Nk/6)\{6x\ln 2x - 3(1-2x)\ln 3 - (6x-2)\ln(6x-2), && \text{for } 1/3 \leq X < 1/2 \end{aligned} \tag{3}$$

Next, we consider the inter-plane disordering. The following scheme is concerned in this process. In the initial state at the absolute zero temperature, the sites A, B and C on the X planes are thought to be statistically occupied by the oxygen atoms,

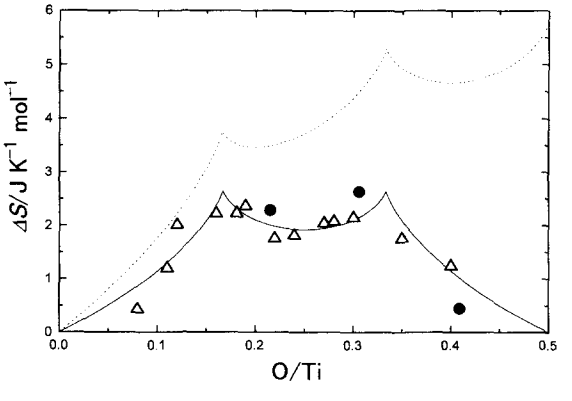

Fig. 13. Transition entropy changes for TiO_x against O/Ti ratio. ————: Eq. (3), · · ·: Eqs. (3) and (4), ●: Tsuji et al. [7,17], △: Koiwa and Hirabayashi [12].

and all the sites on the Y planes to be empty, as schematically illustrated by broken lines in Fig. 5. With increasing temperature, the sites on the Y planes are gradually filled with the oxygen atoms and finally all the sites on both X and Y planes are gradually filled with oxygen atoms and finally all the sites on both X and Y planes are equally occupied above a transition temperature (T_{c2}).

The difference in the configurational entropy changes between the disordered and ordered states is obtained:

$$\Delta S_8 = (Nk/2)\{(1-2x)\ln(1-2x) - 2(1-x)\ln(1-x) + 2x\ln 2\}. \quad (4)$$

The difference in the configurational entropy is easily calculated from Eqs. (3) and (4) for two disordering processes. In Fig. 13, the solid curve shows the calculated results for the intra-plane disordering, and the dotted curve shows the summation for the intra- and inter-plane disordering. The theoretical curves have two maxima at the compositions $x = 1/6$ and $x = 1/3$, consisting with the experimental results obtained by Koiwa and Hirabayashi [18] which are smaller than those obtained by Tsuji and Nakamura [17]. However, the experimental data marked with closed circles and open triangles are quite close to the solid curve than the dotted one. From a theoretical point of view, the above discrepancy may be a consequence of the present over-simplified model. One of the ways to improve the agreement with the experiment is as follows. If the nearest neighbor pairs of oxygen parallel to the c-axis are prohibited to form even in the α-phase at high temperatures as discussed in hafnium –oxygen alloys (the first term in Eq. (1)), the change in the configurational entropy ΔS_8 will be considerably decreased at higher oxygen contents.

References

[1] R. Kikuchi, Phys. Rev. 81 (1951) 988.
[2] T. Tsuji, M. Amaya, Netsu Sokutei 23 (1996) 128, 168.
[3] T.B. Massalski, H. Okamoto, O.R. Subramanian, L. Kacprzak, Binary Alloy Phase Diagrams, 2nd Ed. (ASM International, Metals Park, OH, 1990).
[4] S. Yamaguchi, J. Phys. Soc. Jpn. 21 (1966) 2096.
[5] M. Hirabayashi, Phys. Status Solidi (a)23 (1974) 331.
[6] M. Hirabayashi, S. Yamaguchi, T. Arai, J. Phys. Soc. Jpn. 35 (1973) 473.
[7] T. Tsuji, M. Sato, K. Naito, Thermochim. Acta 163 (1990) 279.
[8] T. Tsuji, M. Amaya, K. Naito, J. Thermal Anal. 38 (1992) 1817.
[9] T. Tsuji, M. Amaya, K. Naito, Thermochim. Acta 253 (1995) 19.
[10] T. Tsuji, M. Amaya, J. Nucl. Mater. 223 (1995) 33.
[11] T. Kato, T. Tsuji, Thermochim. Acta 267 (1995) 397.
[12] M. Koiwa, M. Hirabayashi, J. Phys. Soc. Jpn. 27 (1969) 801.
[13] T. Arai, M. Hirabayashi, J. Less-Common Met. 44 (1976) 291.
[14] K. Naito, H. Inaba, M. Ishida, Y. Saito, H. Arima, J. Phys. E7 (1974) 464.
[15] M. Hirabayashi, M. Koiwa, N. Ito, Sci. Rept. Research Inst., Tohoku Univ., 18A-Suppl, 1966, p. 337.
[16] T. Kato, T. Tsuji, J. Nucl. Mater, to be published.
[17] T. Tsuji, N. Nakamura, unpublished work.
[18] M. Koiwa, M. Hirabayashi, J. Phys. Soc. Jpn. 27 (1969) 807.